International Journal of Research in Engineering and Science (IJRES)
ISSN (Online): 2320-9364, ISSN (Print): 2320-9356
www.ijres.org Volume 14 Issue 11 ǁ November 2026 ǁ PP. 01-07

Development of Chalcogenide-Based Graded Bandgap Thin Film Structure of $ZnOS/Sb_2S_3/Sb_2Se_3$ by Chemical bath deposition technique for Solar Cell Application

James Abumchukwu Ezihe
Department of Physics, Federal University of Technology, P.M.B. 1526, Owerri, Nigeria

Abstract
A tri-layer $ZnOS/Sb_2S_3/Sb_2Se_3$ thin-film structure was successfully fabricated for potential application in heterojunction graded bandgap solar cells. The films were deposited using chemical bath deposition (CBD) technique, which provided a simple and cost-effective fabrication route. The fabricated $ZnOS/Sb_2S_3/Sb_2Se_3$ thin-film structure demonstrated good stability and excellent photon absorption capability over a wide spectral range. Optical analysis revealed high absorbance values in the UV region with an absorbance value of over 80%. X-ray diffraction (XRD) studies revealed that the deposited tri-layer films were amorphous in nature and remained amorphous after annealing. The film material exhibited both direct and indirect bandgap energies. Graded direct bandgap energy obtained for the $ZnOS/Sb_2S_3/Sb_2Se_3$ tri-layer structure ranged from 1.42 - 3.77 eV for as-grown and 1.67 – 3.48 eV for annealed film materials and the indirect graded bandgap energy for as-grown and annealed films were estimated to be 0.67 eV – 3.84 eV and 1.04 eV – 3.74 eV respectively. The elemental composition was confirmed by X-ray fluorescence (XRF) and energy dispersive X-ray (EDX) analyses. Atomic force microscopy (AFM) analysis showed that the root mean square (RMS) surface roughness of the $ZnOS/Sb_2S_3/Sb_2Se_3$ films decreased consistently with increasing annealing temperature. Overall, the graded bandgap characteristic of the $ZnOS/Sb_2S_3/Sb_2Se_3$ thin-film structure makes it a promising candidate for high-efficiency solar cell applications, as it supports effective absorption of photons across a broad range of the solar spectrum.

Key words: *Graded-bandgap, $ZnS/Sb_2S_3/Sb_2Se_3$, CBD, solar cell.*

Date of Submission: 28-10-2026 Date of acceptance: 07-11-2026

I. Introduction

Materials made from combining chalcogens with metals or non-metals are called chalcogenides. If these materials are made in nano scales we refer to them as thin films. Thin films from chalcogenides are promising semiconductors for optoelectronics properties. Chief amongst these film materials is Sb_2Se_3 which has shown about 33% power conversion efficiency (PCE) theoretically [1]. Due to single junction and fix banggap of the existing thin film solar cells of CdTe/CdS, CIGS/CdS and CZTS/CdS which causes thermalization in devices [2], there is a need to investigate and modify materials that will enhance photon absorption and reduce thermalization in devices, tri-layer $ZnS/Sb_2S_3/Sb_2Se_3$ thin film has exhibited wonderful properties that could solve the existing challenges of single junction and fixed bandgap because of the grading nature of the bandgap and multiple junctions which will eventually reduce thermalization when applied in solar cell fabrication. The tri-layer was achieved through chemical bath deposition technique which is inexpensive and reproducible method of thin film production. As the solar energy sector advances toward next-generation photovoltaic solutions, the need to identify abundant, environmentally friendly materials becomes increasingly critical. Sb_2S_3 and Sb_2Se_3, both V-VI group chalcogenides, exhibit promising characteristics, including high optical absorption coefficients ($>10^5$ cm^{-1}) [2], appropriate bandgap ranges (~1.1–1.7 eV) [3], and strong thermal and chemical stability [4]. When zinc sulfide (ZnOS) is introduced as a window or buffer layer alongside Sb-based absorber layers, it enables the creation of a graded bandgap configuration that enhances the separation and collection of photo-generated charge carriers. The scientific literatures on antimony chalcogenides show that the materials have potential to compete in the solar energy market in the foreseeable future due to their low-cost of production, readily available constituents and non-toxic nature of the material [5]. Due to the unique electrical and optical properties of Sb_2Se_3, it is considered as emerging absorber material that can be applied to the next generation solar cells [6].The superstrate CdS/Sb_2Se_3 thin film solar cell structure has shown conversion efficiency of 5.76 % [7] which is low compared to the conversion efficiency of 7.93 % for Sb_2S_3/Sb_2Se_3tandem solar cell [8]. According to Chao and Jiang [9], the recent antimony chalcogenide solar

cells have conversion efficiencies of 7.5 % for Sb_2S_3, 9.2 % for Sb_2Se_3 and 7.82 % for $Sb_2(S,Se)_3$ absorber layers but have deficiency of open-circuit voltage. Notable achievement has been recorded in antimony chalcogenide solar cells technology in the past few years with power conversion efficiency in the order of 10%, which is close to industrial application level [10, 11, 12]. By findings of the same authors, antimony chalcogenides such as Sb_2S_3, Sb_2Se_3 and $Sb_2(S_xSe_{1-x})$ due to their high stability, low cost, abundant elemental constituents, suitable tuneable bandgap, non-toxicity and high absorption coefficient, have emerged as promising solar energy absorber materials.

In this study, we have grown ZnS/Sb_2S_3/Sb_2Se_3 tri-layer by the method of chemical bath deposition for use in solar cell fabrication. The optical, structural and morphological properties were investigated. The band gap of the tri-layer exhibited tuning as shown by the optical analysis. The graded/tuned material will extend solar absorption spectrum, reduce recombination losses, enhance charge transport, improve device stability, reduce thermilization and improve the power conversion efficiency when used in solar cell fabrication [13, 14, 15].

II. Synthesis

The concept of chemical bath deposition (CBD) technique was used to develop ZnOS, Sb_2S_3 and Sb_2Se_3 film materials. This technique is cheap, simple and reproducible in large surface area and can also be achieved in ambience temperature. The procedure for synthesis of ZnOS has been reported in the literature [16]. The procedure for synthesis of Sb_2S_3 has been reported in our previous work [17]. And the synthesis of Sb_2Se_3 thin film has been reported in our work [18]. After optimisation of the film growth processes, the graded structure was fabricated as follows: The window material i.e. ZnOS was deposited on the microscope slide by CBD technique after which the absorbing materials of Sb_2S_3 and Sb_2Se_3 were deposited one after the other by the same method, which resulted to the graded bandgap structure of $ZnOS/Sb_2S_3/Sb_2Se_3$. After synthesis of the materials, they were rinsed in distilled water and dried in air. Thereafter annealed at temperature of 150 ^{0}C.

The structural characterization was achieved with the use of X-ray diffraction and Raman spectroscopy. The XRD measurement was carried out with the Rigaku Smart Lab X-Ray diffractometer with CuK alpha (wavelength = 1.5406 A). The absorbance and reflectance were gotten from the use of Perkin Elmer UV-Vis-NIR spectrophotometer optical measurement system. The characterization was within the UV-Vis-NIR region of the electromagnetic spectrum. The compositional analysis was done using energy dispersive X-ray (EDX) and X-ray fluorescence (XRF). The morphological analysis was done by Stromlingo DIY atomic force microscopy (AFM).

III. Results and Discussion

Figure 1 shows XRD patterns of as-grown and 150 °C annealed ZnOS/Sb_2S_3/Sb_2Se_3 thin films. The patterns showed no diffraction peaks for both as-grown and annealed film materials. It confirmed that the tri-layers remained amorphous after thermal treatment.

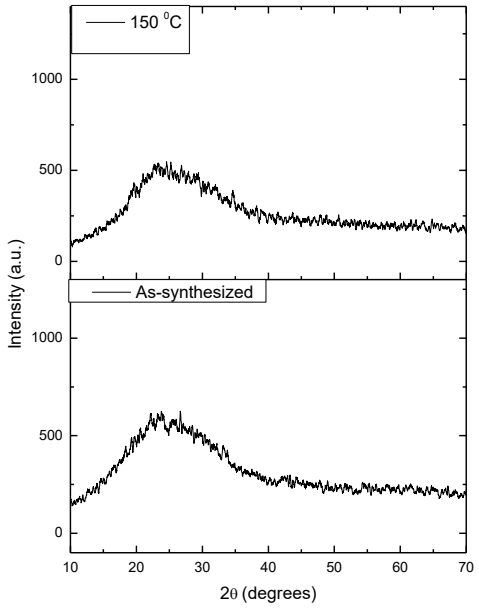


Figure 1: XRD patterns of ZnOS/Sb_2S_3/Sb_2Se_3 thin films

The graph of Figure 2(a) presents a plot of optical absorbance against wavelength for as-deposited and 150 °C annealed $ZnOS/Sb_2S_3/Sb_2Se_3$ thin film structure. From the graph, the absorbance gradually rose from near infrared with a steady value into the visible, at the orange portion of the visible, as-grown and annealed film materials separated, and moved singly into the UV region where they joined again. Annealed film showed higher absorbance than as-deposited in the visible and infrared regions of the solar spectrum. The tri-layer material showed a good absorbance across the solar spectrum.

Figure 2(b) depicts a plot of optical reflectance against wavelength for as-synthesized and 150°C annealed $ZnOS/Sb_2S_3/Sb_2Se_3$ thin film structure. The reflectance of the as-deposited and annealed films rose sharply from the infrared into the visible regions of the spectrum and crosses each other at the red portion of the visible. This high reflectance continued into the UV region of electromagnetic spectrum. It was observed that annealing improved the reflectivity of the material. The high reflectivity of the tri-layer material can be applied in anti-reflective coating for solar panels and displays, in solar cell as backside reflectors for enhanced energy absorption, reflective coatings for thermal radiation shielding, solar reflectors for spacecraft power generation, thin film sensors for environmental monitoring etc.

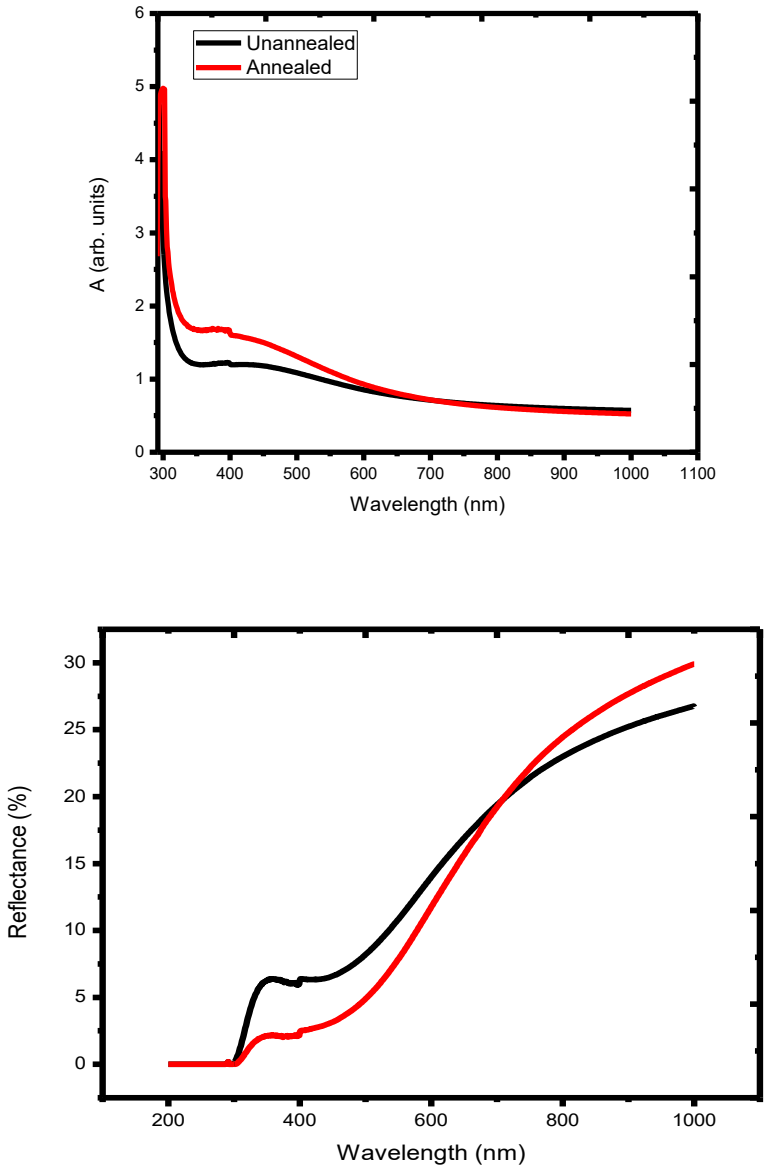


Figure 2: (a) A plot of optical absorbance against wavelength for as-grown and 150 °C annealed $ZnS/Sb_2S_3/Sb_2Se_3$ thin film structure. (b) A plot of optical reflectance against wavelength for as-grown and 150 °C annealed $ZnS/Sb_2S_3/Sb_2Se_3$ thin film structure.

The film material exhibited both direct and indirect bandgap behaviour. Figure 3(a) depicts a plot of direct energy bandgap against photon energy for as-grown and annealed $ZnOS/Sb_2S_3/Sb_2Se_3$ thin film material. Determination of direct band gap energy by the plot of square of absorbance vs photon energy has been reported by some authors in the literature [19-21]. From the figure, the bandgap grading/tuning of as-grown film is in the range of 1.42 eV – 3.77 eV and annealed is 1.67 eV – 3.48 eV respectively. Which reflects the range of energy bandgap values for ZnS, Sb_2S_3 and Sb_2Se_3 respectively [22-29]. From the figure, the tri-layer structure exhibited two absorption edges, i.e $ZnOS/Sb_2S_3$ and Sb_2S_3/Sb_2Se_3. The double absorption edges will ensure enhance charge-carrier mobility, create long charge carrier lifetime, long diffusion length and low exciton binding energy when applied in solar cell production.

Figure 3(b) depicts a plot of indirect energy bandgap against photon energy for as-grown and annealed $ZnOS/Sb_2S_3/Sb_2Se_3$ thin film structure. From the plot the indirect energy bandgaps were estimated using absorbance to power half against photon energy. This method has been reported by [18, 30]. The bandgap grading/tuning for as-grown and annealed films were estimated to be 0.67 eV – 3.84 eV and 1.04 eV – 3.74 eV respectively. Again, these bandgap ranges cover the tuned bandgap of ZnOS, Sb_2S_3 and Sb_2Se_3 thin film materials as have been reported in the literature [31-32]. The bandgap grading/tuning is needed to achieve comprehensive absorption of solar energy. It will ensure absorption of photons from the ultraviolet end to the near infrared end of the solar spectrum and greatly reduce thermilization which is usually witnessed with single junction solar cells.

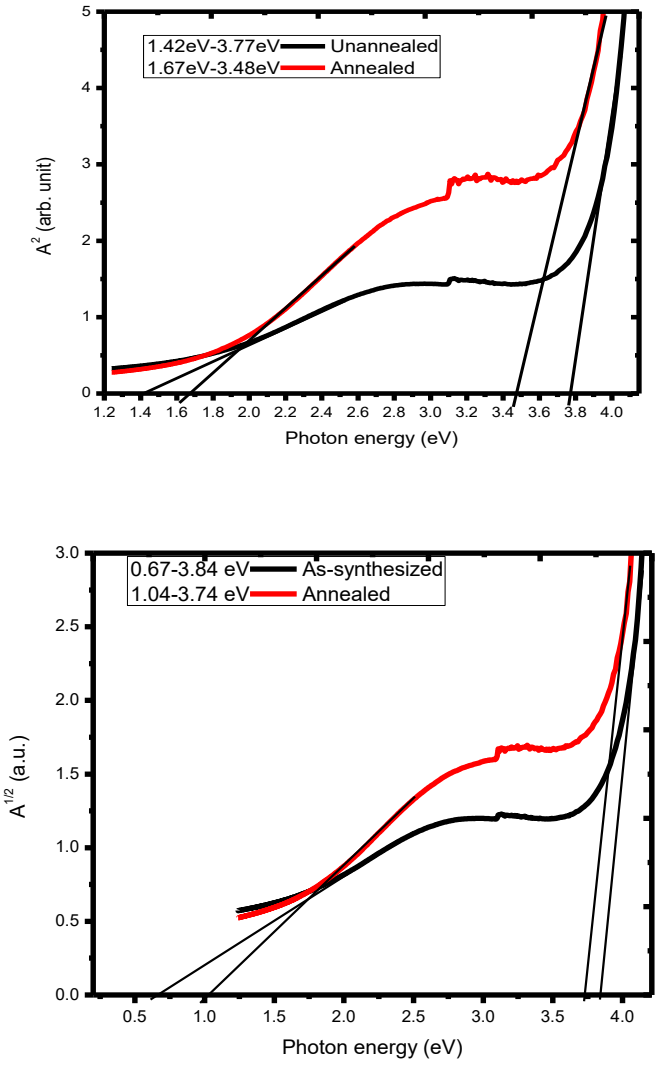


Figure 3: A plot of direct energy bandgap against photon energy for as-grown and annealed $ZnS/Sb_2S_3/Sb_2Se_3$ thin film structure, (b) A plot of indirect energy bandgap against photon energy for as-grown and annealed $ZnOS/Sb_2S_3/Sb_2Se_3$ thin film structure.

The two and three dimensions of the AFM images of as-deposited and annealed $ZnOS/Sb_2S_3/Sb_2Se_3$ thin film material are depicted in figure 4. From AFM statistical quantities RMS roughness decreased with annealing from 112.7 pm for as-grown to 99.7 pm for annealed sample at 150 °C. This again reaffirms that annealing reduces surface roughness of thin film materials. Higher surface roughness can lead to increased scattering of light, reducing the transmittance and reflectance of the film. It can also enhance absorption, particularly in the UV-Vis range, due to the increased surface area and defects.

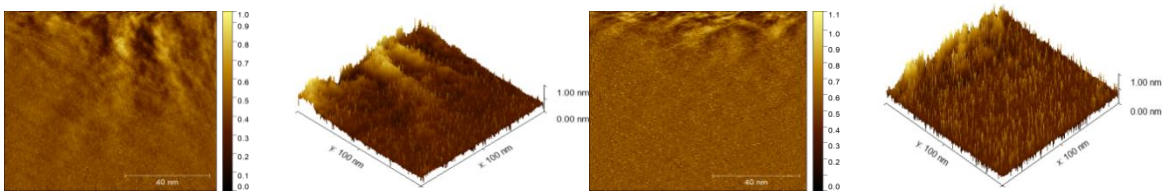


Figure 4: Two and three dimensions of the AFM images of as-deposited and annealed Sb_2Se_3 thin film materials.

The elemental composition was confirmed by EDX and XRF as shown in figure 5. The elements were all confirmed from the XRF analyzer aside sulphur due to its low content, which was confirmed by EDX analysis.

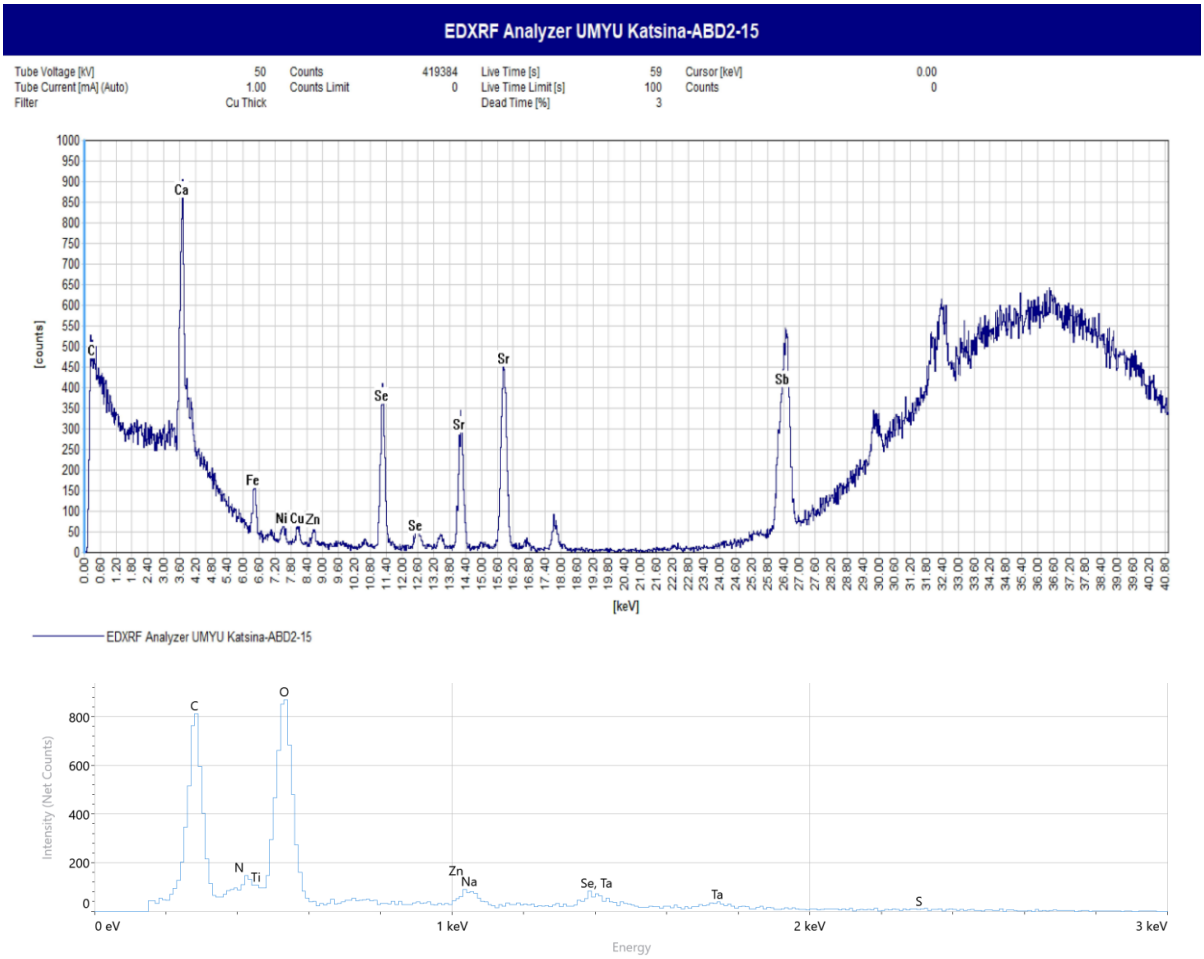


Figure 5: (a) EDX and XRF of $ZnOS/Sb_2S_3/Sb_2Se_3$ thin film

IV. CONCLUSION

By the use of reproducible and cost effective chemical bath deposition technique, we successfully developed $ZnOS/Sb_2S_3/Sb_2Se_3$ thin film tri-layer. Structural characterization via X-ray diffraction (XRD) revealed that the tri-layer thin film of $ZnOS/Sb_2S_3/Sb_2Se_3$ exhibited amorphous behaviour. Optical study revealed that the tri-layer showed both direct and indirect energy bandgap characteristics. Direct bandgap energy

range was 1.42 - 3.77 eV for as-grown film and 1.67 – 3.48 eV for annealed material while the indirect bandgap range was 0.67 eV – 3.84 eV for as-grown film and 1.04 eV – 3.74 eV the annealed sample. The elemental composition was confirmed by energy dispersive X-ray (EDX) and X-ray fluorescence (XRF) analysers. Root mean square (RMS) surface roughness of the ZnOS/Sb_2S_3/Sb_2Se_3 films decreased consistently with increasing annealing temperature according to atomic force microscopy (AFM) analysis. The graded/tuned materials can extend the solar absorption spectrum, reduce recombination losses, enhance charge transport, improve device stability, reduce thermilization and improve the power conversion efficiency when applied in solar cell fabrication.

Acknowledgment: We appreciate our colleagues for their support and assistance.

Conflict of Interest: The author declared that there is no conflict of interest.

REFERENCES

[1] Wang, X.., Kavanagh, S. R., Scanlon, D. O. and Walsh, A. (2024) ‘‘Upper efficiency limit of Sb_2Se_3 solar cells’’ Joule, Vol 8, Issue 7, Pp. 2105-2122. https://doi.org/10.1016/j.joule.2024.05.004.

[2] Ezihe, J. A., Abdulwahab, M., Ezema, F. I. and Echendu, O.K. (2025) ‘‘Essential properties, growth methods, environmental impacts, and solar cell application of antimony triselenide thin films: A review’’ Hybrid Advances, 10 100505. https://doi.org/10.1016/j.hybadv.2025.100505.

[3] Wijesinghe, U., Tetlow, W. D., Maiello, P. Fleck, N., Dowd, G. O., Beattie, N. S., Longo, G. and Hutter, O. S. (2024) ‘‘Crystalline Antimony Selenide Thin Films for Optoelectronics through Photonic Curing’’ Chemistry of Materials, Vol. 36, No. 12, Pp. 6027-6037. DOI: 10.1021/acs.chemmater.4c00540

[4] Luo, Y., Ma, H., Ahmad, N., Shah, U. A., Zheng, Z., Chen, S., Su, Z., Zhao, J., Zhang, X. and Liang, G. (2025) ‘‘ Rapid Thermal-Driven Crystal Growth and Defect Suppression in Antimony Selenide Thin Film for Efficient Solar Cells’’ Nano.MicroSmall, Vol. 2, No.1,1 2403051, https://doi.org/10.1002/smll.202403051

[5] Yong C. C., Sangl il S and Eunjeong H, D.-H. K. (2018) ‘‘Key factors affecting the performance of Sb_2Se_3 – sensitise solar cells during an Se_2S_3 deposition via $SbCl_3$-thiourea complex solution processing’’ JoVE (Journal of Visualised Experiments), e, 58062

[6] Shu, J., Li, Y., Yang, B., Feng, B., Dong, W., Wang, Y., Liang, B., Fan, W., Zhao, X., Li, Z. and Dang, W. (2025) ‘‘Why Sb_2Se_3/CdS Interface Produces Higher Power Conversion Efficiency’’ The Journal of Physical Chemistry Letters, Vol. 16, No. 5 Pp. 1165–1174. doi/10.1021/acs.jpclett.4c03330.

[7] Xin S. L., Xun X., Ye Yang, Ding-Jiang X. and Deng-Bing, L. C. C. (2017). Enhanced Sb_2Se_3 solar cell performance through theory guided defect control. *Progress in* Photovoltaic’s: Research and Applications, Vol. 10, No. 25, Pp. 861–870.

[8] Jianwang Z., Weitao D. L., Yiwei Y., Xiaeomin W. and Reongfeng T. C. (2020) ‘‘All antimony chalcogenide tandem solar cell’’ Solar RRL4, 4, 200048.

[9] Chao C. J. T. (2020) ‘‘Open-circuit voltage loss of antimony chalcogenide solar cells; status, origin and possible solution’’ ACS Energy Letters.

[10] Hongwei L., Jianjun C. and Zuojun T. G. F. (2019) ‘‘Review of recent progress in antimony chalcogenide-based solar cells: Materials and devices’’ Solar RRDL, 6, 13900026

[11] Duan, Z. Liang, X. Feng, Y. Ma, H., Liang, B. Wang, Y., Luo, S. Wang, S. Schropp, R.E.I., Mai, Y. and Li, Z. (2022) ‘‘Sb_2Se_3 Thin Film Solar Cells Exceeding 10% Power Conversion Efficiency Enabled by Injection Vapor Deposition (IVD) Technology’’ Advanced Materials, 34. 10.1002/adma.202202969.

[12] Zhao, Y., Wang, S., Li, C., Che, B., Chen, X., Chen, H., Tang, R., Wang, X., Chen, G. and Wang, T. (2022) ‘‘Regulating Deposition Kinetics via a Novel Additive-Assisted Chemical Bath Deposition Technology Enables Fabrication of 10.57%-Efficiency Sb_2Se_3 Solar Cells’’ Energy Environ. Sci., Vol. 15, Pp.5118–5128. https://doi.org/10.3390/en16196862.

[13] Echendu, O. K. (2014). Thin film solar cells all-electrodeposited ZnS, CdS and CdTe materials. PhD. Thesis*, Sheffield Hallam University, United Kingdom.*

[14] Dharmadasa, I. M., Ojo, A. A., Salim, H. I., and Dharmadasa, R. (2015) ‘‘Next generation solar cells based on graded bandgap device structures utilising rod-type nano-materials’’ Energies 8, 5440–5458. http://dx.doi.org/10.3390/en8065440.

[15] Ojo, A. A. and Dharmadasa, I. M. (2017) ‘‘Analysis of the electronic properties of all electroplated ZnS, CdS and CdTe graded bandgap photovoltaic device configuration’’ Solar Energy, Vol. 158, Pp. 721–727. http://dx.doi.org/10.1016/j.solener.2017.10.042

[16] Lee W. J., Yu J. H., Cho D. H., Hwang T. H., Kang S. J. and Chung Y. D. (2024) ‘‘Effects of $ZnSO_4$ concentration on the high-rate deposition of CBD-Zn (O, S) buffer layer for Cu (In, Ga) Se_2 thin-film solar cells’’ Ceramics International, Vol. 50, 3519

[17] James Abumchukwu Ezihe (2026) ‘‘Development of Sb_2S_3 as a double absorber layer with Sb_2Se_3 by Simple and Low Cost Chemical Bath Deposition Technique for Solar Cell Applications’’ JOIRES Vol. **7** 666

[18] Ezihe, J. A., Abdulwahab, M., Ezema, F. I. and Echendu, O.K. (2025) ‘‘Development of Chalcogenide Sb_2Se_3, Thin Film by Simple and Low Cost Chemical Bath Deposition Technique for Optoelectronics Applications’’ J. Nano & Mat. Sc. Res, Vol. 3, No. 2 (Special Issue, 2025), Pp. 21 – 27. https://doi.org.10.20221/jnmsr.v3i2.35

[19] Ojo, A. A., Salim, H. I. and Dharmadasa , I. M. (2018) ‘‘The influence of ZnS crystallinity on all-electroplated ZnS/CdS/CdTe graded bandgap device properties’’ Journal of Materials Science: Materials in Electronics, Pp. 1-18. http://shura.shu.ac.uk/21662/

[20] Echendu, O. K., Werta, S. Z., and Dejene, F. B. (2018) ‘‘Effect of cadmium precursor on the physico-chemical properties of electrochemically grown CdS thin films for optoelectroniccs devices application: a comparative study’’ Journal of Material Science: Materials in Electronics’’ Vol. 30, Pp. 365-377.

[21] S. Gu, S. Ullah, F. Khan, X. Wang, P. Liu, S. Yang and Chen Y. (2024) ‘‘Recent advances and perspectives on Sb_2S_3 thin-film solar cells,’’ Materials Today Sustainability, vol. 28, (101019), , https://doi.org/10.1016/j.mtsust.2024.101019

[22] Keshav, R. and Mahesha, M.G. (2018). Photoluminescence and Raman spectroscopic analysis of PV deposited ZnS thin films. Materials Research Bulletin Vol. 105*,* Pp. 360–367.

[23] Roy, P., Ota, J. R., and Srivastava, S.K. (2006) ‘‘Crystalline ZnS thin films by chemical bath deposition method and its characterization’’ Thin Solid Films, Vol. 515, Pp. 1912–1917.

[24] Shah, U. A., Chen, S., Mohamed, G., Khalaf, G., Jin, Z., & Song, H. (2021). *Wide Bandgap Sb_2S_3 Solar Cells*. *2100265*, 1–28. https://doi.org/10.1002/adfm.202100265

[25] Avilez Garcia, R.G., Meza Avendaño, C. A., Mou P., Delgado, F.P., and Mathews, N.R. (2016) ‘Antimonysulfide (Sb_2S_3) thin films bypulseelectrodeposition: Effect of thermal treatment on structural, optical and electrical properties’’ Materials Science in Semiconductor Processing, Pp. 4491–100. http://dx.doi.org/10.1016/j.mssp.2015.12.018

[26] Chalapathi, U., Poornaprakash, B. and Park, S. H. (2020) "Influence of post-deposition annealing temperature on the growth of chemically deposited Sb_2S_3 thin films" Superlattices and Microstructures,141106500. https://doi.org/10.1016/j.spmi.2020.106500
[27] Ghosh, S., Moreira, M. V. B., & Gonzalez, J. C. (2020) "Growth and optical properties of nanocrystalline Sb_2Se_3 thin-films for the application in solar-cells" Solar Energy, Vol. 211, Pp. 613–621. https://doi.org/doi.org/10.1016/j.solener.2020.10.001
[28] Mavlonov, A., Razykov, T., Raziq, F., Gan, J., Chantana, J. and Qiao, L. (2020) "A review of Sb_2Se_3 photovoltaic absorber materials and thin-film solar cells" Sol. Energy, Vol. 201, Pp. 227–246.
[29] Chen, C., Li, W., Zhou, Y., Chen, C., Luo, M., and Tang, J. (2015) "Optical properties of amorphous and polycrystalline Sb_2Se_3 thin films prepared by thermal evaporation" Appl. Phys. Lett. Vol. 107, 043905
[30] Olusola, O.I., Madugu, M.L. and Dharmadasa, I.M. (2017) "Investigating the electronic properties of multi-junction ZnS/CdS/CdTe graded bandgap solar cells" Materials Chemistry and Physics, S0254-0584, 30053-6. doi:10.1016/j.matchemphys.2017.01.027
[31] Khatoon, N.F., Aslam, Z., Shoab, M., Ali, J. and Zulfequar, M. (2025) "Temperature-dependent conduction and optical bandgap reduction in Zn-doped thermally evaporated Sb_2Se_3 thin film: a comprehensive investigation" Journal of Materials Science: Materials in Engineering, Vol. 20, No. 1, Pp.130.
[32] Li, P., Xue, F., Fu, B. and Ren, D. (2026) "Potential of Bifunctional SnS to Substitute Spiro for High-Efficiency Full-Inorganic $Sb_2(S, Se)_3$ Solar Cells With n-i-p Configuration" Energy Technology, Vol. 14, No. 8, Pp.e70615.